JOURNAL OF MATERIALS SCIENCE 29 (1994) 632–639

Acoustic emission data on delayed damage processes in the vicinity of defects in fibre-reinforced plastics

A. P. TISHKIN, G. N. GUBANOVA, A. M. LEKSOVSKI
A. F. Ioffe Physical-Technical Institute, Russian Academy of Sciences, Politechnicheskaya 26, 194 021, St. Petersburg, Russia

V. E. YUDIN
Institute of Macromolecular Compounds, Russian Academy of Sciences, Bolshoy 31, 199 004, St. Petersburg, Russia

Analysis of the time intervals between acoustic emission (AE) signals in composites makes it possible to study defect mechanisms induced by stress transfer near the previously arisen defect. Unidirectional carbon fibre-reinforced plastics (CFRP) with matrices of different plasticity have been investigated during tensile deformation. There is a characteristic delay time, τ_1, between the correlated appearance of defects. For these materials, τ_1 ranges from 50–500 μs. In the model considered here, τ_1 is determined by the time for which the zone of plastic deformation formed at the place of fibre breaking and widening during local stress relaxation, is extended to the neighbouring fibres. Thus, the fibre is overloaded, which may lead to its breaking. The effect of viscoelastic properties on τ_1 is discussed. This delay time decreases with the plasticity of the matrix. These data also show that the zone of localized deformation at the broken fibre can cover several layers of neighbouring fibres.

1. Introduction

The failure of fibre composite materials is a result of damage accumulation in material during loading. In many cases it may be considered that defects can interact. Hence, to understand the transition from diffuse damage accumulation to catastrophic failure, the study of correlated defect formation is of considerable interest. Generally speaking, fibre-reinforced plastics (FRP) exhibit such different defect types as fibre breaking, cracks in the matrix, debonding on the fibre–matrix interface, and delamination between plies. In order to calculate composite strength, the breaking of several neighbouring fibres should be given particular attention because subsequent fibre breaking may lead to avalanche-like failure. The usual approach is to calculate the stress transfer from the broken fibre to the neighbouring fibres using the Weibull distribution of fibre strength [1–3], and also any irregularity of fibre packing should be taken into account [4]. It has been shown [5] that not only static stress transfer should be taken into account but also the dynamic overload. This overload in the breaking plane on fibres neighbouring the broken fibre is approximately twice as large as in static analysis. A still greater value of stresses is obtained if the possibility of the appearance of a crack in the matrix around the broken fibre is taken into account, while, in contrast, debonding increases the fracture energy of the developing defect, thus hindering the development of group fracture. This model for group fracture formation has been described elsewhere [6]. From the same considerations, it follows that it is important to take into account correlated defect appearance (including defects of different types), not just when the final fracture of the composite is determined by the avalanche-like fibre fracture. Thus, when the delamination crack is developed, a damage zone is formed at its tip and the development of defects at the tip provides a contribution to the fracture energy [7].

In all these cases it was assumed that stress transfer around the defect that leads to the appearance of other defects takes place for the time which is comparable to that of the passage of elastic stress waves through the local volume considered, i.e. in the range from nanoseconds to several microseconds. In this work we shall attempt to show that the contribution to correlated defect formation is also provided by the slower process of stress transfer. This process is due to the relaxation of stress around the defect, and, correspondingly, to the overloading of neighbouring volumes that increases in the case of the localization of plastic deformation of the polymer matrix. In this case, the CFRP structure is relatively regular, and therefore characteristic delay times exist between the appearance of defects, ranging from several tens of microseconds to a few milliseconds.

Defect appearance was recorded by the method of acoustic emission (AE). The spectral and energetic analysis of AE signals was also carried out. In certain limits it permits identification of signal sources.

0022–2461

TABLE I Physico-mechanical properties of the binders for CFRP

Binder	Tensile strength (MPa)	Shear modulus (GPa)	Ultimate elongation (%)	Specific work of fracture[a] (MPa)	T_g, (°C)
PEI	90–100	0.9–0.95	10–12	0.6–0.9	210
PEI-N	40–50	1–1.2	3–4	0.04–0.06	260
EDT-10	70–90	0.95–1.1	6–8	0.2–0.3	85

[a] In this case, the specific work of fracture is the area under the stress–strain line.

2. Materials and methods

2.1. Properties of the materials of the matrix and the composite

CFRP based on ELUR carbon band with fibre diameter 10 μm with thermoplastic and thermosetting matrices were investigated. A polyesterimide binder (PEI) based on benzene dianhydride and diphenylsulphone diamine was used as the thermoplastic matrix. Oligomer ester imides based on the same dianhydrides and diamines were also used as thermosetting binders. They contain norbornane end groups (PEI-N) which make it possible to obtain a three-dimensional cross-linked polymer. Additionally, an epoxy EDT-10 binder was used as a thermosetting binder. At room temperature this binder is more brittle than PEI but more plastic than PEI-N (Table I).

PEI synthesized as a solution in methylpyrrolidone and oligomers synthesized in chloroform were deposited on a carbon fabric, the solvent was evaporated and the prepregs were pressed forming eight-layer plastics. The main characteristic of carbon plastics based on this binder are listed in Table II.

The specimens for tensile tests were plates 200 mm long, 15 mm wide, and 1–1.5 mm thick. The loading rate was 0.22 mm min^{-1} and the typical fracture time was 8–10 min.

2.2. Acoustic emission techniques

AE signals were recorded by a piezotransducer with a frequency band up to 650 kHz and after amplification and filtration (50 kHz–2 MHz) were digitized by a transient data recorder (model 4604 with a memory of 1 kB and transferred to the computer to save in the magnetic disk. In spectral analysis the sampling period was 0.25 μs and the sampling frequency was 4 MHz (Nyquist frequency 2 MHz). In this case, after the input signal exceeds the set trigger level, the data sampling time is 256 μs. This time may be longer or (less frequently) shorter than the signal duration. Moreover, several signals can occur in this time period, and the analysis of this situation is the main subject of this work. Hence, we will distinguish the concept of the AE signal and the "realization" as a result of digitizing the input signals (AE signals and noise background) for the whole time of digitizing. Lower sampling frequencies, 250 kHz (digitizing time 4096 μs) and 1 MHz were also used for the analysis of the occurrence of several signals in the "realization". Examples of realizations with different sampling frequencies are shown in Fig. 1a–c. About 100 realizations were recorded for each experiment. In some cases, up to 1000 realizations were recorded.

TABLE II Physico-mechanical properties of CFRP

Binder	Tensile strength (MPa)	Shear modulus (GPa)	Fibre volume fraction (%)
PEI	800–840	4.4	46
PEI-N	900–1010	5.4	62
EDT-10	1000–1090	5.7	58

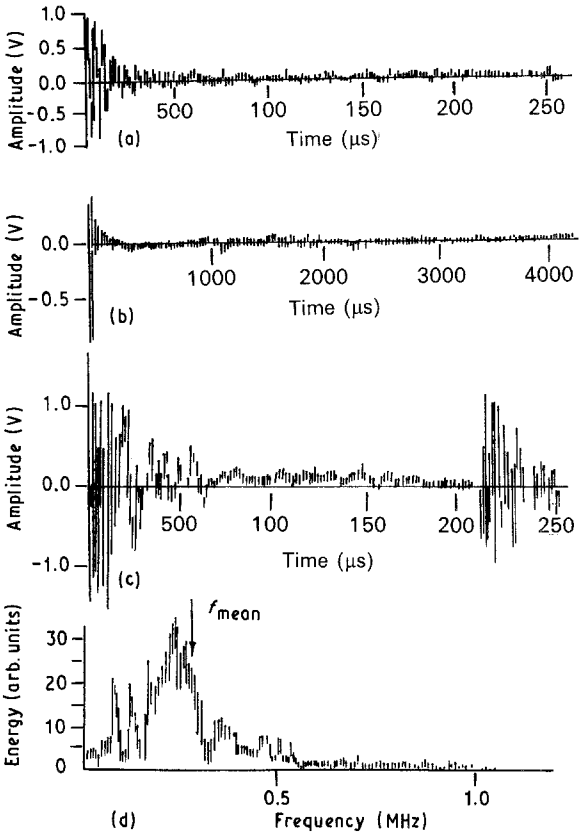

Figure 1 Examples of realizations of AE signals and energy spectrum.

During treatment the energy spectrum of the signal (realization) and its mean frequency were calculated by fast Fourier transform (Fig. 1d). The spectrum was used to determine the realization energy, W, in the range 50–1000 kHz and in five narrower frequency bands. The noise energy of the measuring system in the selected frequency ranges is automatically subtracted.

A more usual recording system of AE events and their amplitudes was simultaneously used. This system

works under conditions of linear location of signal sources coordinates. In this case, two transducers were used with a resonant frequency of 450 kHz. It should be noted that no signals from the region of the specimen grips were detected.

3. Results and analysis

3.1. Characterization of AE in CFRP with different matrices

AE in the fibre composites has been investigated in many papers, e.g. [8–15]. Much attention was devoted to the possibility of AE signal separation according to their source type. This problem is solved more simply in composites that exhibit no delamination. In this case, the amplitude of signals of fibre failure is higher (at least on average) than that of other defects [8]. Hence, by increasing the discrimination level, AE may be recorded from fibres alone, and the kinetics of accumulations of their breaks may be studied [9, 10]. Signal amplitude from large delamination cracks may be comparable to or larger than that in fibre failure. In this connection it is reasonable to use AE spectral analysis [11–13]. However, so far, this analysis has seldom given clear results and in any case gives no universal results. Therefore, in some cases the methods of pattern recognition that are relatively formal from the physical standpoint, should be used [12, 14]. Delayed AE was studied by Rochat *et al.* [15] during creep, but they have not considered any effects of the defect's localization.

In the present work, the AE spectral analysis was carried out both for the above-mentioned composites and for model specimens with a single carbon fibre in the epoxy matrix. When model specimens were stretched, fibres were fragmented and the number of fragmentations approximately corresponded the number of AE signals. Fig. 2 shows the distribution of mean frequencies of realizations for the composites under investigations, and Fig. 3 shows energy distributions. It is clear that both CF/PEI composites and the model composite exhibit no signals with such high-energy values as the two other composites, and the mean frequency distribution is narrower. Judging from specimen fracture surfaces, in CF/PEI-N and CF/epoxy the delamination process is very developed in contrast to that in CF/PEI. As can be seen from Table I, this is in agreement [16] with specific work of fracture of the corresponding binders. Hence, if the data on the model composite are taken into account, it may be suggested that AE signals in the CF/PEI composite are mainly due to fibre fragmentation. In the other CFRP considered here the contribution of signals from delamination cracks is considerable. The size of these cracks can differ greatly and, hence, the energy and frequency characteristics of the signals also vary. The region of the lowest energies should also be noted. Their fraction in CF/PEI is higher than in single fibre fragmentation. Some of these signals may be due to debonding.

3.2. Analysis of time interval distributions between AE signals

The spectral characteristics considered above reflect the dynamics of defect development at velocities close

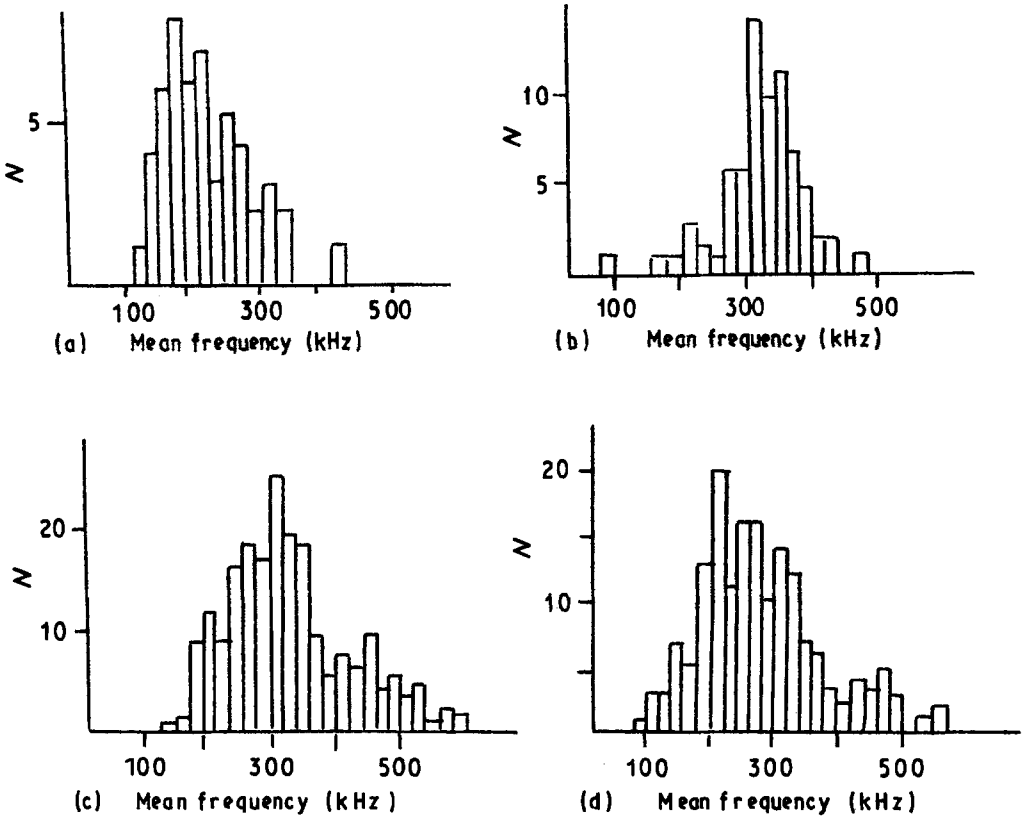

Figure 2 Distributions of mean frequency for AE realizations. (a) Model composite, (b) CF/PEI, (c) CF/PEI-N, (d) CF/epoxy.

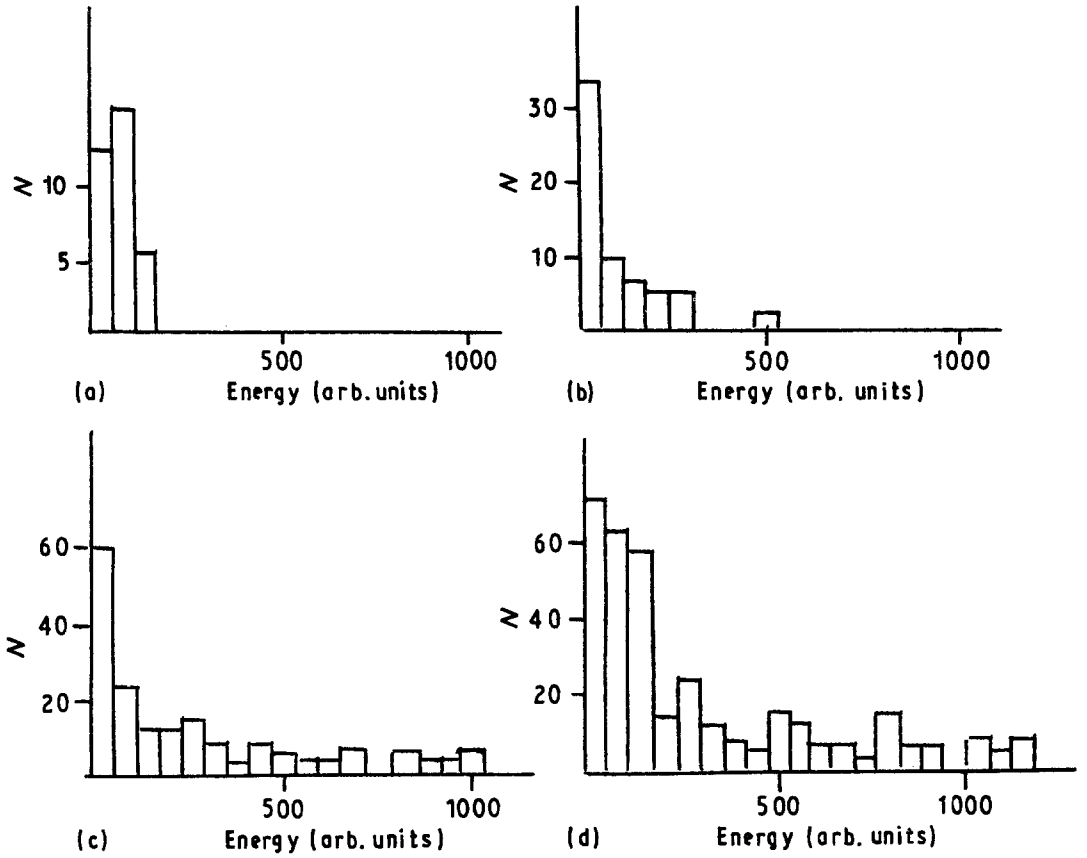

Figure 3 Distributions of energy for AE realizations. (a) Model composite, (b) CF/PEI, (c) CF/PEI-N, (d) CF/epoxy.

to sound velocities. The time range of these processes does not exceed a few microseconds, for example the process of elastic stress transfer after carbon fibre fragmentation continues for several tens of nanoseconds [5]. During the same time range, the process of correlated break of a fibre group can occur. Because this range is less than the response time of the AE recording instruments, only one AE signal with the energy proportional to the number of fibre fragmentation will be fixed [9]. However, the AE investigations both in homogeneous materials and composites show that correlated defect generation is also observed at much longer time intervals between the appearance of these defects, although they are small compared to the loading rate when the increase in loading on the specimen may be neglected [17–19]. In this situation the AE signals from different defects do not merge into one event, and the existence or absence of correlation is determined in the framework of the theory of a stochastic point process from the analyses of time intervals between the signals (events), τ. The process of independent events may be described as the Poisson process with the intensity λ. For this process the distribution function, $f(\tau)$, of time intervals between the events is $f(\tau) = \lambda\exp(-\lambda\tau)$ [20]. For the AE process, λ is equal to event rate $\dot{N}$, and in many cases this process can actually be described as the Poisson process [17, 18]. The appearance of correlation between the AE events can most often be represented [18] in the form of a cluster Poisson process (Neyman–Scott process) [21, 22]. In this case each event of the primary Poisson process can lead to a certain secondary process. This is reflected in interval distribution in the form of an increase in $f(\tau)$, as compared to the Poisson distribution at low τ.

Fig. 4 shows the distribution of time intervals between the AE events for the CF/epoxy composite obtained with AE recording system of the events. In some loading stages the distribution may be considered to be the Poisson distribution. However, the investigated CFRPs are characterized to a greater extent by the existence of differences in the Poisson distribution with sufficient statistics at $\tau < 10$–50 ms, i.e. by the existence of partial correlation between defect formations.

This AE system makes it possible to investigate the complete flow of AE events but its lower resolution limit is about 1 ms. The recording of AE by the transient data recorder make it possible to investigate the time intervals from 20 μs (a typical decay time of the signal from fibre break to the level when the next signal can be distinguished on its background) to

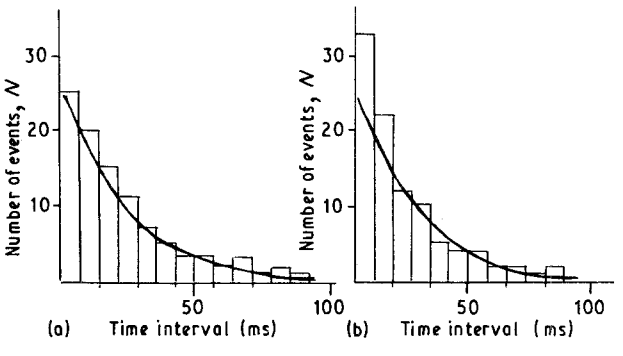

Figure 4 Examples of time interval distributions for AE events.

256 μs or 4 ms, depending on sampling frequency. In fact, for CFRP there is a set of realizations with two or more signals in them (Fig. 1c) (in realization with a length of 256 μs more than two signals are present very seldom). Hence, although only a part of the AE flow is investigated by this method, in principle it permits the study of the "fine structure" of clusters in the cluster Poisson process. The existence of such clusters can be seen in Fig. 4b. Note that the second signals in the realizations of the type shown in Fig. 1c are not reflected signals and can be easily distinguished from them by their short rise time.

The distributions of time intervals between AE signals in the realizations for CFRP with different matrices are shown in Figs 5–8. The occurrence of two signals in one realization naturally does not mean the correlated appearance of sources of these signals. It is possible to estimate the probability of random grouping of signals in one realization from the AE event rate if the entire AE flow is considered to be the Poisson flow. Such an estimation for the CF/PEI-N composite shows, for realizations with a duration of 256 μs (which are the more interesting for this composite) that this probability is negligible in any stage of specimen loading. In the CF/PEI and CF/epoxy composites, the realizations with a duration of 4 ms are more informative and at a final stage of deformation this event rate can exceed 100 events/s. Thus in Figs 5 and 6 the fraction of intervals between non-correlated events may be high. A more definite estimation is difficult because the AE process is not stationary. However, all these distributions fundamentally differ from the Poisson process distribution by the existence

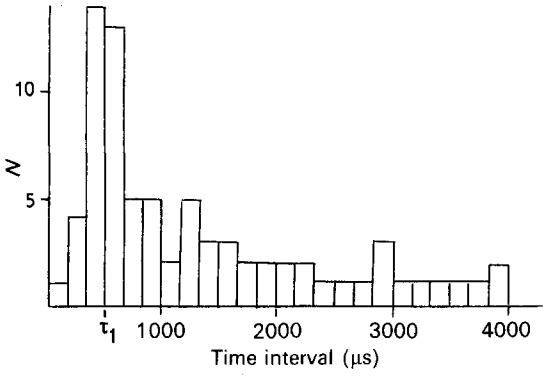

Figure 5 Time interval distribution for AE signals inside AE realizations in CF/PEI composite.

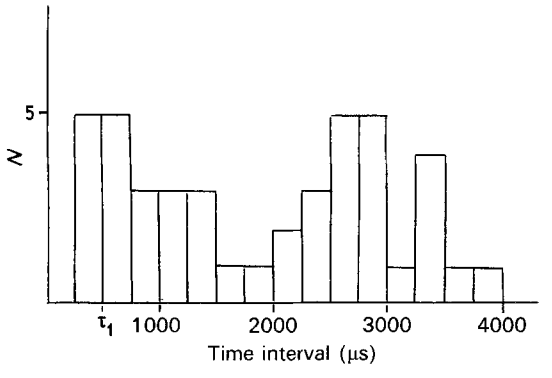

Figure 6 Time interval distribution for AE signals inside AE realizations in CF/epoxy composite.

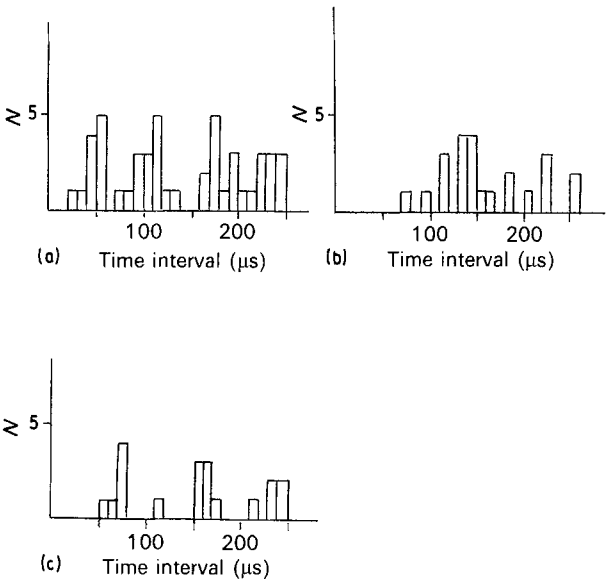

Figure 7 Time interval distributions for AE signals inside AE realizations in CF/PEI-N composites. (a) $\sigma < 600$ MPa, (b) $\sigma > 600$ MPa, (c) another batch.

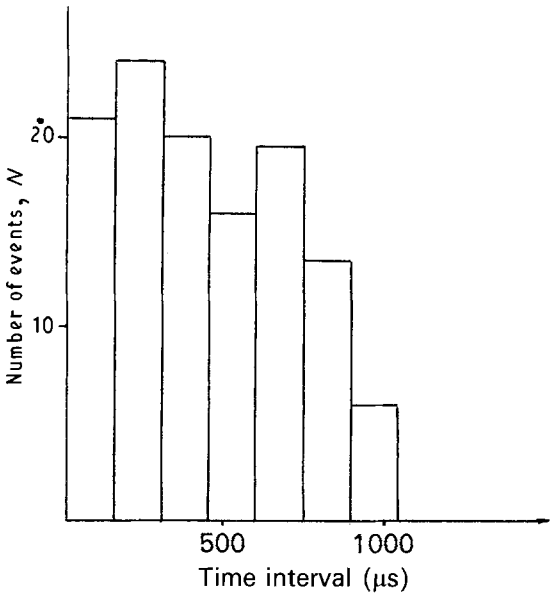

Figure 8 Time interval distribution for AE signals inside AE realizations with 1024 μs sampling time (CF/PEI-N).

of at least one maximum. For the CF/PEI composite the distribution maximum is at $\tau_1 = 500$ μs (Fig. 5), and in CF/PEI-N the first maximum is at $\tau_1 < 100$ μs (Fig. 7a, c). In the CF/epoxy composite, τ_1 could be estimated as 400 μs.

Interval distributions for the CF/PEI-N composite (Fig. 7a, b) are plotted for two loading stages, the boundary between which is determined by the stress $\sigma = 600$ MPa.

The probability of the appearance of correlated AE signals in CF/PEI is approximately 25%–40%, and in CF/epoxy 15% (for realizations with a duration of 4096 μs) and in CF/PEI-N, this 4%–5% (for realizations 256 μs).

4. Discussion

Let us consider the mechanism according to which the arising of one defect may lead to the arising of another

defect for the times longer than those characteristic for elastic stress transfer, but sufficiently small for increasing in specimen loading to be neglected.

It was shown elsewhere [18] for the interaction between twins in zinc, that the secondary process (cluster) generated by the appearance of a large twin may, in turn, be described as the Poisson process of non-interacting events with decreasing intensity. This corresponds to the following model: defect formation leads to an abrupt increase in local stress and plastic deformation rate, $\dot{\varepsilon}$, which relax according to the exponential law or a similar law to the average level of the whole sample. To the first approximation, the probability of the appearance of a new defect in unit time may be considered to be proportional to $\dot{\varepsilon}$. This leads to the above relationship for the secondary process, and a probability maximum of interval distribution is at $\tau \to 0$.

In these interval distributions between AE signals in CFRP, the maximum is displaced from zero. Hence, this model should be altered. It is natural to think that for fibre composites this shift in τ is determined by the average distance between fibres that form a relatively regular structure. We will now assume for preciseness that the defects, and especially the first defects in clusters, are fibre fragmentation (it should be remembered that in these materials clusters mostly consist of two AE signals, i.e. of two defects). This assumption is adequate at least for CF/PEI. Stress relaxation near a broken fibre is usually considered from the standpoint of a stress transfer along the broken fibre [23, 24]. However, it is known that a crack formed in fibre fragmentation can develop further in the matrix. It has been shown by high-speed photography [25] that after the crack passes a certain distance almost at sound velocity, it does not stop instantaneously, and during the stage of relaxation its velocity begins to decrease. In fact, crack growth in this stage is related to the necessity for crack opening displacement at its tip, δ, from the value of δ_0, which corresponds to the dynamic crack growth up to the value of δ_{st}, which is the equilibrium value at this load. Hence, it is possible to use the usual equations of stress relaxation where stress will be changed by δ

$$\delta(\tau) = \delta_0 + (\delta_{st} - \delta_0)\,[1 - \exp(-\alpha\tau)] \quad (1)$$

where α is the relaxation parameter. We will assume that the size of the plastic zone at the crack tip, as in homogeneous materials, linearly depends on δ [26] and that the shape of the zone cross-section is circular and its area increases from R_0 to the equilibrium value R_{st} (Fig. 9a). An equation analogous to Equation 1 will be valid for $R(\tau)$. The distance between the neighbouring fibres is denoted by L, and for simplicity it is assumed that R_0 and the crack length are small compared to L. Then the time, τ_1, after which the plastic zone reaches the nearest fibre, is given by

$$\tau = \frac{1}{\alpha}\ln\frac{R_{st}}{R_{st} - L} \quad (2)$$

Note that R_{st} is the final zone length in the matrix material and not in the composite.

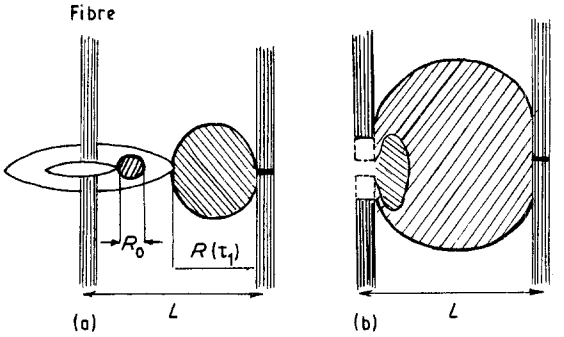

Figure 9 Model for delayed secondary fibre break (a) with and (b) without matrix cracking near the primary fibre break.

Theoretical and experimental data show that in composites the plastic zone at the tip of a crack which intersects fibres is greatly extended in the fibre direction [27]. Our data do not contradict this but indicate that in addition to a "diffuse" plastic deformation zone, a zone of large local deformations appears either in the crack plane (analogous to the Dugdale model [28]) or forms an angle with it as shear bands. Plastic deformation abruptly increases at the boundary of this zone. The rate of plastic deformation at the place of the probable defect formation has a maximum at the passing of the zone front, i.e. after the time, τ_1, with respect to primary fibre fragmentation. This leads to the appearance of a maximum in time interval distributions (Fig. 5). Although plastic deformation is absent in PEI-N in tensile tests, this do not implies that plastic deformation is absent under other loading conditions [29] or in a local volume at a stress concentrator [27].

In interval distributions for CF/epoxy (Fig. 6) and, in particular, for CF/PEI-N (Fig. 7) composites, not only one but at least two maxima are observed. On the basis of the model under consideration, this implies that the zone of localized deformation is not limited by the nearest fibre layer and, in spite of relatively dense fibre packing, proceeds in several layers. Moreover, the distribution of distances from the fibres to the central fibre being destroyed retains the short-range order in two or three layers. For CF/PEI-N we have τ_i = 50, 105, and possibly 170 and 230 μs (Fig. 7a) and for another sample batch we have τ_i = 75, 160, and possibly 240 μs (Fig. 7c). At higher τ, single maxima are no longer distinguished, but in any case the time intervals between correlated AE signals reaches 1000 μs (Fig. 8). Therefore, it may be assumed that R_{st} in CF/PEI-N is higher than the distance to the fourth fibre layer. Then for the first three layers, Equation 2 passes into an almost linear dependence of the τ_i on the distance to a fibre in the ith layer, L_i. If τ_i is expressed in relative units, $\tau_i^0 = \tau_i/\tau_1$, then one obtains virtually integer series and, correspondingly, an integer series for $L_i^0 = L_i/L_1$. If the fibres were packed in squares, we would have the following series for L_i^0:1, 1.4, 2, ... However, the data reported here are in a favour of circular fibre packing.

Consideration of CFRP with different matrices shows that a decrease in τ_1 and an increase in the number of distribution maxima take place with decreasing matrix plasticity. In the explicit form, visco-

elastic properties of the material influence the τ_1 value in Equation 2 via the coefficient α and the R_{st} value, for which direct data are not available. However, it is clear that in a less plastic material, R_{st} is also lower. Hence, the expected influence of this parameter on τ_1 is opposite to the observed trend. It is more complex to evaluate the effect of α. In the usual relaxation models [30], the relaxation parameter is mainly determined by the plastic deformation rate at the moment of onset of relaxation, $\dot{\varepsilon}(0)$. This value, in turn, depends on effective stress, $\sigma^*(0)$. The thermal activation character of deformation is given by

$$\alpha = A \exp\left[- \frac{\Delta G_0 - v^*\sigma^*(0)}{kT} \right] \quad (3)$$

where A is the coefficient, ΔG_0 is the change in free energy in the absence of stress, v^* is the activation volume, k is the Boltzmann constant and T is the absolute temperature. In this paper, relaxation processes at the crack tip are considered on the basis of Equation 1. Hence, it may be assumed that the initial crack opening, δ_0, is the initial condition that determines α. According to fracture mechanics, the value of δ_0 is determined by the value of effective surface energy, γ_{eff}, and α may be qualitatively expressed instead of Equation 3 by

$$\alpha = C\exp(W/\gamma_{eff}) \quad (4)$$

where C and W are constant. Some idea about the γ_{eff} value for different materials may be obtained from Table I on specific work of fracture.

The considerations leading to Equation 4 are not rigorous but they explain qualitatively the decrease in τ_1 with decreasing matrix plasticity.

It should be borne in mind that in a plastic material (in particular, in PEI) a crack in the matrix may not appear after fibre break, but the development of a plastic zone near the breaking place will proceed (Fig. 9b). In this case, the role of crack opening is played by the distance between the ends of broken fibres. This change in the micromechanics of the process leads to a decrease in both α and R_{st} and, hence, to an increase in τ_1 (as compared with the model shown in Fig. 9a) and to a decrease in the degree of deformation localization. The decrease in the degree of deformation localization in CF/PEI and CF/epoxy composites as compared to CF/PEI-N (as a result of a change in matrix plasticity and/or a change in the micromechanics of the process) leads to the broadening of peaks of interval distribution and to a considerable decrease in the probability of correlated defect appearance for the second and following fibre layers. The appearance of time intervals, τ, exceeding 200 μs between the arising of defects in CF/PEI-N may be caused by either the spreading of the zone of localized deformation to more distant fibre layers, or by the accumulation of deformation in the diffuse zone at the nearest environment of the broken fibre. The reason for the change in range distribution in this composite that occurs a short time before failure (Fig. 7b) is not yet clear. However, it is somehow related to the increase in the fraction of delamination cracks in this loading stage.

5. Conclusions

It has been shown for unidirectional CFRP on the basis of the statistical analysis of time intervals between AE signals that:

1. in the consideration of the mechanisms of group (correlated) defect generation, particularly fibre breakage, it is necessary to take into account the stress relaxation process occurring near the defect. This process decreases stress in this volume and, hence, increases it in neighbouring volumes, mainly as a result of the broadening of the zone of localized plastic deformation. Consequently, the probability of failure of several neighbouring fibres is greater that it follows from the analysis of stress transfer near the broken fibre in elastic approximation.

A more detailed consideration permits the following conclusions to be drawn.

2. Because fibre packing in the composite is relatively regular, there is a characteristic delay time between the correlated failure of neighbouring fibres, τ_1.

3. The zone of localized plastic deformation developing from the place of fibre break can include several neighbouring fibre layers, especially in a composite in which the matrix exhibits low plasticity.

4. The delay time between the breakage of single fibres, τ_1, decreases with the plasticity of the matrix material, varying from 50–500 μs for the composites considered here.

The spectral analysis of AE showed that in the composites in which delamination proceeds actively, the distribution of mean frequencies of AE signals is broader than that in composites in which the process of fibre fragmentation predominates.

Acknowledgement

The authors thank V. M. Svetlichniy, PhD, Institute of Macromolecular Compounds, Leningrad, for supplying polyesterimide samples.

References

1. C. ZWEBEN, *AIAA J.* **6** (1968) 2325.
2. C. ZWEBEN and B. W. ROSEN, *J. Mech. Phys. Solids* **18** (1970) 189.
3. R. E. PITT and S. L. PHOENIX, *Int. J. Fract.* **22** (1983) 243.
4. S. OCHIAI and K. OSAMURA, *J. Mater. Sci.* **24** (1989) 3536.
5. A. S. OVCHINSKIJ and E. N. SAKHAROVA, *Mech. Kompos. Mater. (USSR)* **4** (1981) 620.
6. V. S. KRIVOBODROV and A. M. LEKSOVSKI, *ibid.* **6** (1987) 999.
7. K. FRIEDRICH, R. WALTER, L. A. CARLSSON, A. J. SMILEY and J. W. GILLESPIE Jr, *J. Mater. Sci.* **24** (1989) 3387.
8. J. BECHT, H.-J. SHWALBE and J. ELSENBLATTER, *Composites* **7** (1976) 245.
9. A. M. LEKSOVSKI, in "Deformation and fracture kinetics of composite materials", edited by S. P. Nikanorov and A. M. Leksovski (FTI, Leningrad, 1983) p. 112 (in Russian).
10. I. NARISAWA and H. OBA, *J. Mater. Sci.* **19** (1984) 1777.
11. R. L. MECHAN and I. V. MULLIN, *J. Compos. Mater.* **5** (1971) 266.
12. K. YAMAGUCHI, H. OYAIZU, K. KUDOH and Y. NAGATA, "Progress in Acoustic Emission III" (Japanese Society NDI, Zao, 1986) p. 594.

13. A. OKADA, T. YASUJIMA and T. TAZAWA, *Trans. Jpn Inst. Metals* **28** (1987) 1004.
14. M. CHEFAROUI, J. ROGET, A. LEMASCON and M. JEANVILLE, in "Proceedings of 6th International Conference on Composite Materials (ICCM-VI/ECCM-2)", London, July 1987, Vol. 1, edited by F. L. Matthews, N. C. R. Buskell, J. M. Hodgkinson and J. Morton (Elsevier, London, 1987) p. 424.
15. M. ROCHAT, R. FOUGERET and P. FLEISCHMANN, *J. Acoust. Emission* **9** (1990) 91.
16. M. R. PIGOTT, *J. Mater. Sci.* **23** (1988) 3778.
17. A. P. BRAGINSKIJ, in "Fracture Physics and Mechanics of Composite Materials", edited by A. M. Leksovski (FTI, Leningrad, 1986) p. 35 (in Russian).
18. A. P. TISHKIN and A. M. LEKSOVSKI, *Pis'ma v ZhTF* **14** (1988) 1463 (in Russian).
19. A. M. LEKSOVSKI, G. N. GUBANOVA, N. A. SUKHANOVA and G. H. NARZULLAEV, in "Physics of Strength of Composite Materials", edited by A. M. Leksovski (FTI, Leningrad, 1988) p. 69 (in Russian).
20. D. R. COX and A. W. LEWIS, "The statistical analysis of series of events" (Methuen, London, 1966).
21. J. NEYMAN and E. L. SCOTT, *J. Roy. Statist. Soc. B* **20** (1958) 1.
22. D. VERE-JONES, *ibid.* **32** (1970) 1.
23. J. M. LIFSHITZ and A. ROTEM, *Fibre Sci. Technol.* **3** (1970) 1.
24. A. ROTEM and J. BARUCH, *J. Mater. Sci.* **9** (1974) 1789.
25. A. M. LEKSOVSKI, A. ABDUMANONOV, R. M. AKHUNOV, G. H. NARZULLAEV and A. P. TISHKIN, *Mekh. Kompos, Mater.* **6** (1984) 1004.
26. D. BROEK, "Elementary Engineering Mechanics", 3rd Edn (Martinus Nijhoff. The Hague, 1984).
27. S. L. BAZHENOV and A. A. BERLIN, *J. Mater. Sci.* **25** (1990) 3941.
28. D. S. DUGDALE, *J. Mech. Phys. Sol.* **8** (1960) 100.
29. C. G'SELL, D. JACQUES and J. P. FAVRE, *J. Mater. Sci.* **25** (1990) 2004.
30. V. I. DOTSENKO, *Phys. Status Solidi (b)* **93** (1979) 11.

Received 11 September 1991
and accepted 2 September 1992